processes

MDPI

Article

The Influence of Complementary Processing Methods to Emulsification on the Sunscreen Emulsion Properties

Yasmin R. Santos [1], Newton Andreo-Filho [1], Patricia S. Lopes [1], Daniele R. Araujo [2], Anderson F. Sepulveda [3], Caroline C. Sales [1], Andre R. Baby [4], Marcelo D. Duque [1] and Vânia R. Leite-Silva [1,5,*]

[1] Departamento de Ciências Farmacêuticas, Instituto de Ciências Ambientais, Químicas e Farmacêuticas, Universidade Federal de São Paulo (UNIFESP), Diadema 09913-030, SP, Brazil; yasmin.rosa@unifesp.br (Y.R.S.); newton.andreo@unifesp.br (N.A.-F.); patricia.lopes@unifesp.br (P.S.L.); caroline.cianga@unifesp.br (C.C.S.); marcelo.duque@unifesp.br (M.D.D.)
[2] Department of Biophysics, Paulista Medical School, Universidade Federal de São Paulo (UNIFESP), São Paulo 04023-062, SP, Brazil; daniele.ribeiro@unifesp.br
[3] Natural and Human Sciences, Federal University of ABC, Santo André 09210-580, SP, Brazil; anderson.sepulveda@ufabc.edu.br
[4] Department of Pharmacy, Faculty of Pharmaceutical Sciences, University of São Paulo, Sao Paulo 05508-000, SP, Brazil; andrerb@usp.br
[5] Frazer Institute, Faculty of Medicine, The University of Queensland, Brisbane, QLD 4102, Australia
* Correspondence: vania.leite@unifesp.br

Abstract: Different processing conditions to produce emulsions can modify the dispersion of ingredients, visual aspect, and viscosity, influencing the final product's effectiveness. In this study, a primary sunscreen emulsion was produced by the conventional stirring process and subsequently subjected separately to complementary processing methods. A Box-Behnken 2^3 factorial design was applied to each complementary processing method: the High-Shear Method (CP-HS) and the High-Pressure Homogenization Method (CP-HPH). The present study aimed to investigate the influence of these complementary processes on particle size distribution (PSD), Zeta potential, pH, rheological properties, in vitro SPF, and photostability. In the CP-HS factorial design, the factors explored at three levels were stirring speed and stirring time, while in the CP-HPH design, the factors varied at three levels of pressure and the number of cycles through the high-pressure homogenizer. Results indicated that both complementary processing methods significantly influenced ($p < 0.05$) the physicochemical characteristics of the primary sunscreen emulsion, which was applied as the starting point. In CP-HS, the sample subjected to 15,000 rpm for 15 min exhibited the highest in vitro SPF ($p < 0.05$), with an average value of 42 at T0, while the primary sunscreen emulsion had an SPF of 30. In CP-HPH, a more pronounced reduction and uniformity in PSD among the studied methods were observed ($p < 0.05$), and the range of data was 0.20–0.34 µm. These results emphasize how different processing methods can influence the final characteristics of an emulsion and where suitable choices can significantly benefit the product.

Keywords: emulsion complementary process; ultra-turrax; high-pressure homogenizer

check for updates

Academic Editor: Paolo Trucillo

Received: 9 May 2024
Revised: 18 June 2024
Accepted: 8 July 2024
Published: 13 February 2025

Citation: Santos, Y.R.; Andreo-Filho, N.; Lopes, P.S.; Araujo, D.R.; Sepulveda, A.F.; Sales, C.C.; Baby, A.R.; Duque, M.D.; Leite-Silva, V.R. The Influence of Complementary Processing Methods to Emulsification on the Sunscreen Emulsion Properties. *Processes* **2025**, *13*, 520. https://doi.org/10.3390/pr13020520

Copyright: © 2025 by the authors. Licensee MDPI, Basel, Switzerland. This article is an open access article distributed under the terms and conditions of the Creative Commons Attribution (CC BY) license (https://creativecommons.org/licenses/by/4.0/).

1. Introduction

Emulsions consist of a dispersion of two immiscible phases and are present in various products in the cosmetic, pharmaceutical, and food segments [1,2]. Considered thermodynamically unstable, they tend to undergo phase separation through phenomena such as creaming, coalescence, coagulation, or Ostwald ripening [3,4]. Understanding the phenomena that cause instability in the system is an important step, where aspects such as the

concentration and physical-chemical properties of the components, emulsification method, particle size distribution, and storage conditions can be responsible for intense structural changes in the emulsion [5,6].

When there is no balance in the emulsified system, gravitational separation probably occurs by the density difference between phases (sedimentation or cremation) [3,4]. Coalescence occurs due to the absence of coverage of the particles, where there is no barrier to continuous phase approximation, leading to irreversible phase separation [7–9]. Coagulation occurs when the particles present an anomalous level of approximation caused by changes in particle charges, generating aggregates [10]. Ostwald ripening is related to the decrease or disappearance of the smallest particle size population due to the high energy they need to stabilize, while larger particles increase spontaneously, as it is a process that demands less energy and tends to enhance thermodynamic stability [11,12].

In this context, much research has investigated the performance of various ingredients in different concentrations and combinations to achieve physicochemically stable emulsions [13–17]. In addition to exploring different ingredients and their combinations, processing methods should also be explored. The choice of processing method plays an essential role in enhancing a thermodynamically unstable system to show kinetic stability over the shelf-life [3,18,19].

The input of mechanical energy to obtain emulsionated systems leads to the dispersion of particles within the external phase of the system. The distribution, interaction, and uniformity of particles are essential for understanding the physicochemical aspects and sensory attributes of emulsions [19,20]. A consistent reduction in the particle size distribution (PSD) during processing significantly contributes to the improved physicochemical stability of emulsions. The employment of high-energy and high-shear processes, in addition to emulsification, is an alternative approach for refining and ensuring uniformity in PSD [21,22].

The mechanical device based on the rotor-stator principle is widely used to fragment, rearrange, and reduce particles through the high-shear method (CP-HS). The equipment is composed of an internal rotor that achieves high-speed stirring levels and an external stator, with a small distance between both structures ranging from 100 to 3000 μm [23]. The mechanical device increases the shear stress rate within the dispersion, leading to an increased energy dissipation rate. This is facilitated by the specific geometry and short distance between the rotor and stator positions. High-shear energy and the promotion of dissipation contribute to the refinement and uniformity of emulsion systems through the breakdown and rearrangement of particles [20,23,24].

In complementary processing methods, smaller and uniform particles can also be achieved through the High-Pressure Homogenization Method (CP-HPH). This technique is based on the high-energy concept and is widely used to obtain submicron emulsions and nanoemulsions [25,26]. In this method, the emulsion undergoes high-pressure homogenizer (HPH), where the mechanical force exerted by high-pressure pistons facilitates emulsion passage through a narrow gap. The high shear of the turbulent flow and the oscillation induced by the applied pressure (cavitation) produce a smaller and more uniform particulate system. Given their in-line dispersion design, emulsions can be subjected to one or more cycles [27,28].

In this study, a sunscreen emulsion was initially produced by a conventional stirring process as the starting point. Subsequently, complementary processing by high-shear (CP-HS) and high-pressure (CP-HPH) were separately applied, with parameters defined by factorial design. The impacts of each complementary processing on the physicochemical, organoleptic, and performance properties of a sunscreen emulsion formula were evaluated before and after stress conditions.

2. Materials and Methods

2.1. Reagents and Chemicals

Dicaprylyl Carbonate, Bis-Ethylhexyl Metoxyphenyl Triazine, and Diethylamino Hydroxybenzoyl Hexyl Benzoate were purchased from BASF (São Paulo, Brazil), Ethylhexyl Methoxycinnamate, Butyl Methoxydibenzoylmethane, Potassium Cetyl Phosphate, Sodium Stearoyl Glutamate, and Tocopheryl Acetate were purchased from DSM (São Paulo, Brazil); Glycerin, Disodium EDTA, and Butylatedhydroxytoluene were purchased from LabSynth (São Paulo, Brazil); Xanthan Gum was purchased from CP Kelco (São Paulo, Brazil); Cetyl Alcohol was purchased from Dinamica Química Contemporânea (São Paulo, Brazil); Caprylyl glycol (and) Ethylhexylglycerin were purchased from Proserv Química (São Paulo, Brazil), and Polyacrylate Crosspolymer-11 was purchased from Clariant (São Paulo, Brazil).

2.2. Emulsions Processing

A primary sunscreen emulsion was produced to serve as a starting point for the proposed methods. After all production (primary emulsion and both complementary processing methods), all resulting assays were analyzed at T0 and after 3 freeze-thaw cycles, in which the samples were submitted to 40 °C/24 h and then to −18 °C/24 h for 6 days (Figure 1).

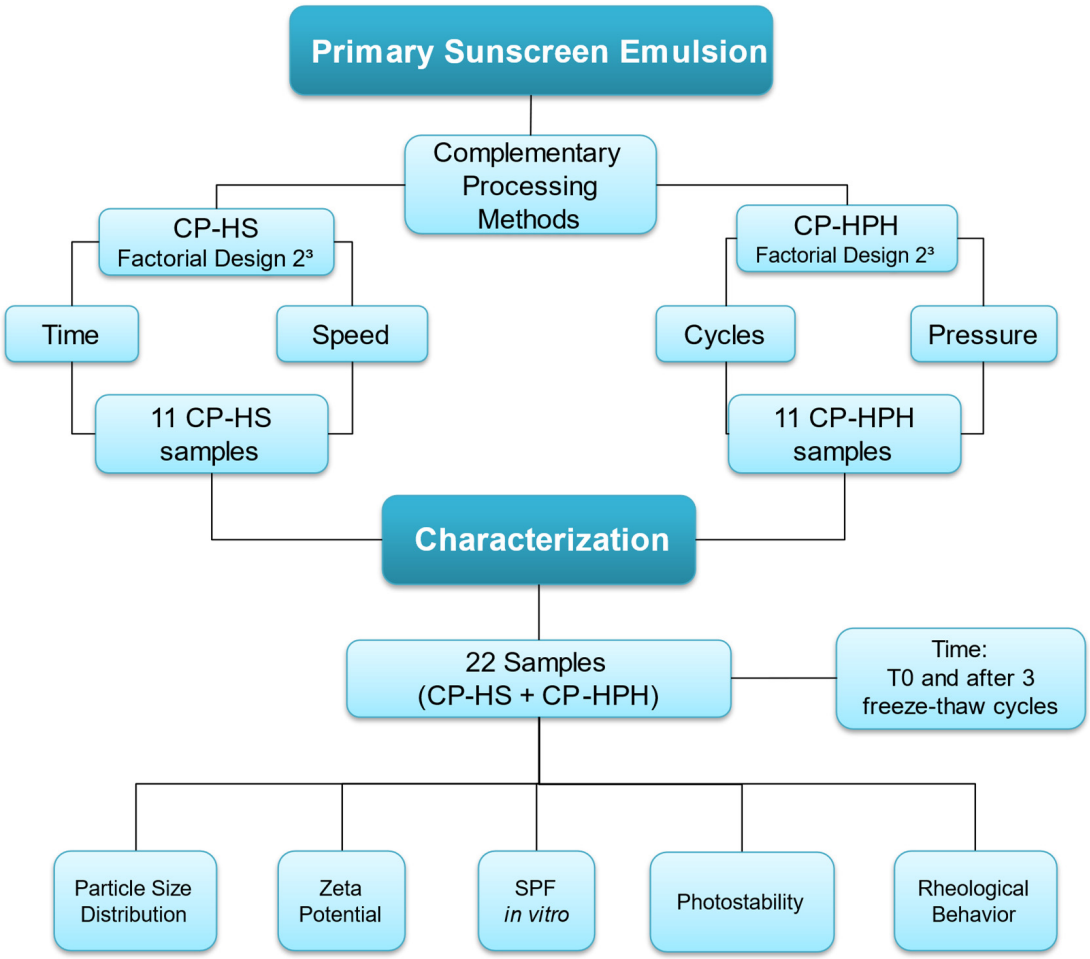


Figure 1. Flowchart of the steps performed in the current study, from the initial production to the evaluation of the final characteristics at the initial time (T0) and after three freeze-thaw cycles.

2.2.1. Primary Sunscreen Emulsion

The emulsion used as a starting point was produced with the components listed in Table 1. The hydrophilic components in the primary sunscreen emulsion are the polar (water miscible) ingredients, which compose the aqueous phase, and the lipophilic ingredients (water immiscible), representing the oil phase (see "Polarity" column). These components form an unstable thermodynamic system without the presence of amphiphilic ingredients like Potassium Cetyl Phosphate and Sodium Stearoyl Glutamate, which stabilize the emulsion by allowing the immiscible phases to mix through interfacial tension reduction.

Table 1. Primary sunscreen emulsion composition.

Phase	Ingredient	Function	*w*/*w* (%)	Polarity
A	Glycerin	Humectant	5.00	Polar
	Xanthan Gum	Rheological modifier	0.20	Polar
	Aqua	Vehicle	59.39	Polar
	Disodium EDTA	Chelating	0.06	Polar
B	Dicaprylyl Carbonate	Emollient	10.00	non-Polar
	Butylated hydroxytoluene	Antioxidant	0.05	non-Polar
	Bis-Ethylhexyloxyphenol Methoxyphenyl Triazine	UV filter	5.50	non-Polar
	Ethylhexyl Methoxycinnamate	UV filter	8.00	non-Polar
	Butyl Methoxydibenzoylmethane	UV filter	2.00	non-Polar
	Cetyl Alcohol	Viscosity controlling	1.00	non-Polar
	Diethylamino Hydroxybenzoyl Hexyl Benzoate	UV filter	4.00	non-Polar
	Potassium Cetyl Phosphate	Surfactant	2.50	Amphiphilic
	Sodium Stearoyl Glutamate	Surfactant	0.40	Amphiphilic
C	Tocopheryl Acetate	Antioxidant	0.50	non-Polar
	Caprylyl Glycol (and) Ethylhexylglycerin	Multifunctional emollient	0.60	non-Polar
D	Polyacrylate Crosspolymer-11	Rheological modifier	0.80	Amphiphilic

In a jacketed tank with a 10 kg capacity mixer (Lemaq Industrial e Comercial Analítica, São Paulo, Brazil) at 600 rpm, Phase A (aqueous phase) was dispersed at room temperature and heated at 80 °C. Then, Phase B (oil phase), previously heated at 80–85 °C, melted and homogenized, was included in the tank under stirring. After 15 min, the heating was turned off, and the emulsion was stirred until the system reached below 50 °C. Phase C (antioxidant and emollient components) was added and homogenized. Subsequently, the stirring speed was increased to 800 rpm, and Phase D (rheological modifier) was slowly added until complete dispersion. The primary sunscreen emulsion was prepared and divided separately for submission to complementary processing methods.

2.2.2. Complementary Processing by High-Speed Method (CP-HS)

The preparation of emulsions by CP-HS was conducted using different speed and stirring time conditions with the Ultra-Turrax® T-18 Basic equipment (IKA Works GmbH & Co. KG, Staufen, BW, Germany). The conditions were planned through a full 3^2 factorial design using the Statistica® software version 12.0 (StatSoft Inc., Tulsa, OK, USA). Rotations

(level: 5000, 10,000, and 15,000 rpm) and stirring times (level 2: 3, 7, and 15 min) were selected as factors, with two repetitions of the central point, as shown in Table 2.

Table 2. Experimental conditions for CP-HS, obtained through a full 3^2 factorial design.

Sequence of Experiments	Speed (rpm)	Time (min)	Formulation Code
4	5.000	7	4-HS
6	15.000	7	6-HS
5	10.000	7	5-HS
10	10.000	7	10-HS
8	10.000	15	8-HS
11	10.000	7	11-HS
9	15.000	15	9-HS
2	10.000	3	2-HS
7	5.000	15	7-HS
3	15.000	3	3-HS
1	5.000	3	1-HS

For each experiment, 150 g of primary sunscreen emulsion was placed in a 250 mL becker (6.0 cm diameter), and the probe of the high-shear equipment was introduced in the center of the sample formulation. Stirring was initiated from zero until the settled speed for the first 30 s at room temperature. After reaching the settled speed, the beaker was moved elliptically to ensure that the stir probe would reach every part of the formulation.

2.2.3. Complementary Processing by High-Pressure Homogenization Method (CP-HPH)

The emulsions subjected to CP-HPH were prepared using a High-Pressure Homogenizer Nano DeBEE® (Pion Inc. (UK) Ltd., East Sussex, England), where the pressures (levels: 5000, 10,000, and 15,000 psi) and number of cycles (levels: 3, 5, and 7) were employed as factors in the full 3^2 factorial design, with two repetitions of the central point (Table 3).

Table 3. Experimental conditions for CP-HPH obtained through a full 3^2 factorial design.

Sequence of Experiments	Pressure (psi)	Number of Cycles	Formulation Code
4	5.000	3	4-HP
6	15.000	3	6-HP
5	10.000	3	5-HP
10	10.000	3	10-HP
8	10.000	5	8-HP
11	10.000	3	11-HP
9	15.000	5	9-HP
2	10.000	1	2-HP
7	5.000	5	7-HP
3	15.000	1	3-HP
1	5.000	1	1-HP

For each CP-HPH experiment, 150 g of primary sunscreen emulsion was processed in a high-pressure homogenizer at room temperature. The pressure level was adjusted according to the experiment number, and the counter-pressure was maintained at 2000 psi for all experiments.

2.3. Evaluation of Emulsions (Primary Sunscreen Emulsion, CP-HS, and CP-HPH)

The physicochemical and organoleptic properties were initially assessed in a primary sunscreen emulsion, and 22 samples were developed using the CP-HS and CP-HPH methods. Initially, 24 h after production, the emulsions were subjected to centrifugation (Sorvall R6+ Thermo Fisher Scientific, Waltham, MA, USA) for 30 min at 3000 rpm to evaluate the centrifugation resistance of the emulsified system [29]. The characterization of the remaining analyses took place at T0 and after the freeze-thaw cycles.

2.3.1. Evaluation of Particle Size Distribution (PSD) by Static Light Scattering (SLS)

PSD was analyzed using the CILAS 1190 Particle Analyzer, based on the SLS principle. The samples were previously diluted in distilled water (the same dispersant as the equipment) and carefully introduced into the particle analyzer cell under agitation until the obscuration level reached approximately 15%. The Lorenz-Mie theory was applied as the measurement principle, and the analysis was performed in triplicate [30].

2.3.2. Evaluation of Zeta Potential

Zeta Potential was characterized using the Zetasizer Nano ZS equipment (ATA Scientific Instruments, Sydney, Australia). The assessment of the electrophoretic mobility of samples was conducted at 25 °C, following the appropriate dilution of the samples in distilled water (1:10,000). The samples were then subjected to an electric field formed by a pair of electrodes, and all measurements were performed in triplicate [31].

2.3.3. Evaluation of pH Value

After 24 h of processing the primary sunscreen emulsion and the CP-HPH and CP-HS emulsions, the pH was determined using a pH/mV meter 21 HANNA (HANNA instruments, Padova, Italy) at T0 and after the freeze-thaw cycles by direct immersion of the electrode. All measurements were performed at a sample temperature of 25 °C.

2.3.4. Rheological Behavior of Emulsions

The rheological properties of the samples were assessed by rotational moduli in the Kinexus Lab. Oscillatory Rheometer (Malvern Instruments, Worcestershire, UK) with cone-plate geometry and the data were acquired using the rSpace for Kinexus software version 1.61.1968 and analyzed with GraphPad Prism 5 software.

The flow behavior of the samples was evaluated at T0 and after freeze-thaw cycles, where the ascending and descending curves were plotted as a function of shear rate (0.01–100 1/s). The rotations could predict the fluid condition through the Ostwald model (Equation (1)):

$$\tau = K \cdot (\gamma)^n, \quad (1)$$

where flow index = n, consistency index = K, shear rates, and shear stress are represented by γ and τ, respectively [32].

2.3.5. Evaluation of Photoprotective Property and Photostability

In Vitro Sun Protection Factor (SPF)

In vitro SPF analyses were conducted according to Hübner et al., 2023, and Cândido et al., 2022 [33,34]. Each sample was analyzed in triplicate using a diffuse reflectance spectrophotometer with an integrated sphere (UV-2000 Ultraviolet Transmittance Analyzer, North Sutton, NH, USA). On a molded polymethyl methacrylate plate (50 × 50 mm) with a roughness of around 6.0 µm (Helioplate PMMA Molded HD 6, HelioScreen, Creil, France), 32.5 mg of each formulation was applied in circular motions from the edge toward the center, forming a film containing 1.3 mg/cm^2. The weight of each plate was measured

before and after the application to ensure that the correct amount was applied. The samples were then allowed to dry at room temperature and were protected from light for 20 min. Absorbance values were recorded at a wavelength of 290–400 nm, at a scan speed of 1 nm/s, and converted into in vitro SPF values by the UV2000 software, version 1.1.1.0.

In Vitro Photostability

After in vitro SPF analysis, the plates were subjected to a stress condition by artificial radiation to evaluate the emulsions' photostability. The artificial radiation was emitted by a Suntest CPS+ climatic chamber at 580.08 W/m^2–2088 J/m^2 for 1 h at 35 °C, corresponding to a radiation dose of approximately 2089 kJ/m^2. The in vitro SPF of the plates was evaluated in triplicate after irradiation [35].

2.3.6. Statistical Analyses

The influence of factors and levels of CP-HS and CP-HPH, as outlined in Tables 2 and 3, on dependent variables (PSD, Zeta potential, rheological behavior, and in vitro SPF) was assessed using Statistica 12.0 software (StatSoft Inc., Tulsa, OK, USA). For each variable, the statistical model (with linear and quadratic linear interactions) that showed an R^2 value closest to 1 was selected. The results of the dependent variable analyses were evaluated by mean, standard deviation, and ANOVA using Statistica 12.0 and GraphPad Prism 5 (GraphPad Software Inc., San Diego, CA, USA).

3. Results

3.1. Evaluation of Emulsions

Emulsions were obtained through a conventional (primary sunscreen emulsion) method, and both complementary processing methods remained intact without evidence of phase separation at T0 and after centrifugation. Notably, the emulsions from CP-HS and CP-HPH exhibited a lighter coloration in comparison to the primary sunscreen emulsion. This effect is typically elucidated by the PSD reduction, provided by high-shear methods, as well as an increase in the particle population in the system. These changes can influence aspects such as the final coloration of the emulsions [36].

Emulsion systems can be susceptible to physicochemical changes due to extrinsic conditions. In the case of freeze-thaw cycles (FT), despite being an efficient stability test, massive temperature variations can cause significant changes in emulsions [37]. After FT, the CP-HS samples did not show noticeable macroscopic modifications. While emulsions produced with higher pressure levels (10,000 and 15,000 psi) and a higher number of cycles (2 and 3 cycles) in CP-HPH exhibited initial signs of instability, indicating that the lower pressure level—5000 psi—was more stable under the high-temperature variation that samples were subjected to freeze-thaw cycles.

3.2. Evaluation of Particle Size Distribution by Static Light Scattering (SLS)

Data related to the particle surface and distribution are essential for understanding the inherent stability of the physicochemical characteristics of an emulsion [10]. When subjecting the primary sunscreen emulsion to complementary processing methods, a statistically significant reduction ($p < 0.05$) in PSD was found (Figure 2), showing the influence of CP-HS and CP-HPH. Emulsions obtained by complementary processing methods and primary sunscreen emulsion showed a distinct PSD compared to T0; in some cases, it was statistically different ($p < 0.05$).

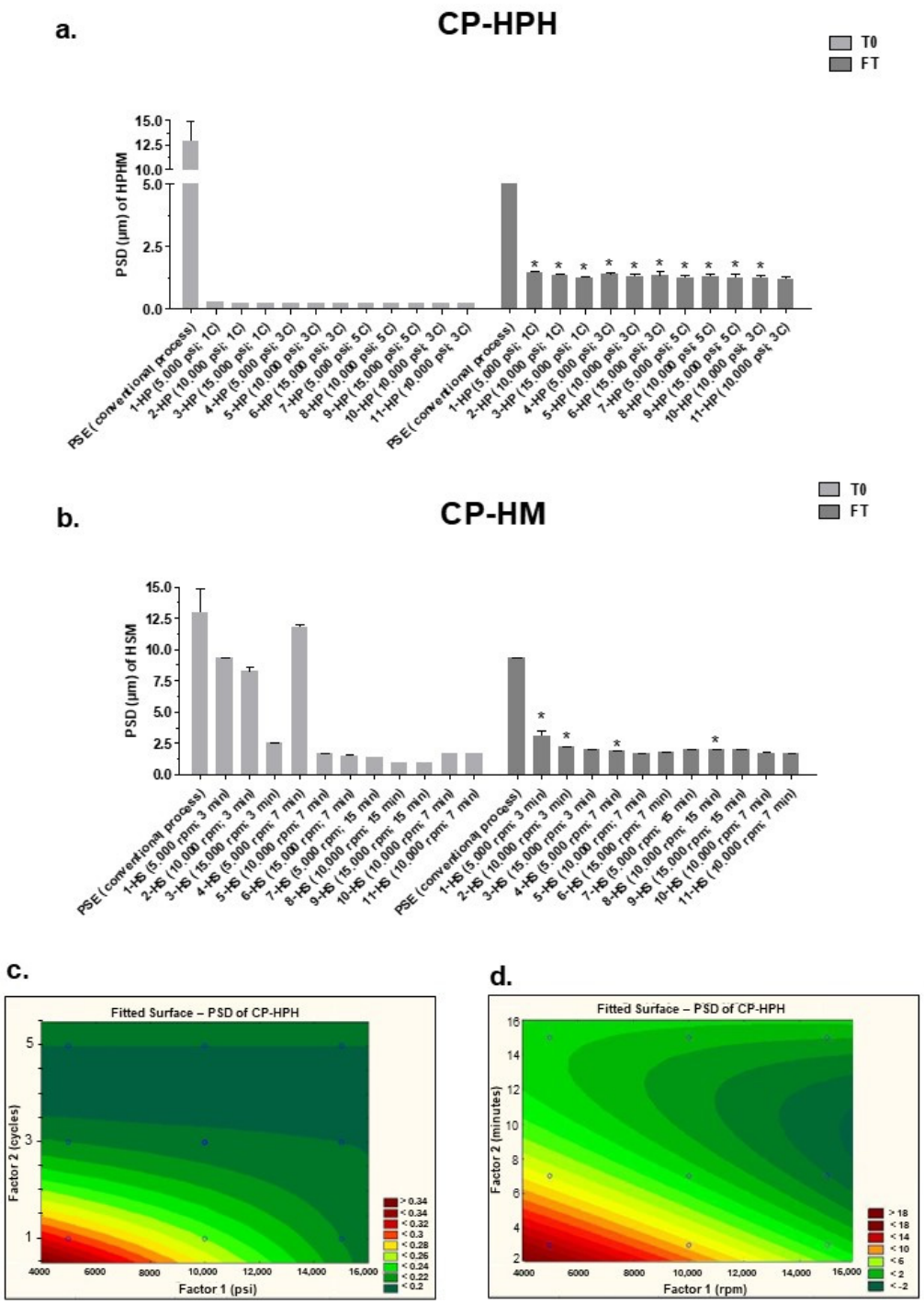


Figure 2. PSD of primary sunscreen emulsion (PSE), CP-HPH (**a**), and CP-HS (**b**) at T0 (initial time) and FT (3 freeze-thaw cycles, resulting in 06 days), where statistical differences ($p < 0.05$) between T0 and FT for each assay are represented by (*), and surface plots (DoE) illustrating the PSD at T0 based on the factors "pressure" and "number of cycles" for CP-HPH (**c**) and "stirring speed" and "stirring time" for CP-HS (**d**). The process conditions used for each sample are indicated in the legend in parentheses at T0, where "C" represents the number of cycles in HPH.

In Figure 2a, CP-HPH shows a higher PSD reduction power when compared to CP-HS. Among the assays of CP-HPH, despite the levels of "pressure" and "number of cycles" factors, the reduction in PSD was linear. After freeze-thaw cycles, the PSD reduction in CP-HPH resulted in phase separation in the assays where the highest levels of the factors of DoE were used, like 3 and 5 cycles, and 10,000 and 15,000 psi.

In CP-HS assays, samples also showed a reduction in PSD at T0 (Figure 2b), where 7-HS, 8-HS, and 9-HS, produced with the highest level of "stirring time" factor (15 min), presented the most notable PSD reduction. 3-HS, 6-HS, and 9-HS assays, which were produced from the highest level of "speed" factor (15,000 rpm, with stirring times of 3, 7, and 15 min, respectively), showed a gradual reduction in PSD at T0, where PSD became smaller with increasing stirring time. In the same way, the lowest level of the "speed" factor (5000 rpm) exhibited similarities, where the reduction in PSD was improved when the stirring time was longer.

The surface plots from the DoE of both methods showed the influence of the independent variables on the PSD. In Figure 2c, the DoE conducted for CP-HPH showed influence on PSD (R^2 = 0.9932), where the factors "pressure" and "number of cycles" had statistically significant differences ($p < 0.05$), indicating different levels of both factors can generate distinct PSD results, also synergy between factors was observed, indicating influence on PSD ($p < 0.05$). Although the PSD results in CP-HPH have some linearity, the variations proposed by DoE can produce particles between 0.20–0.34 µm from the primary sunscreen emulsion (whose mean value was 12.92 µm in T0). CP-HPH reached a plateau for particle reduction capability, as observed in other works [38–40] in the dark green region of the surface plot represented by 4 and 5 numbers of cycles and produced particles of 0.20 µm regardless of "pressure" factor variation.

Emulsions subjected to high shear in rotor-stator devices typically display an average diameter of 1–10 µm [41], supporting the data in Figure 2d. The responses obtained for the levels of independent variables in CP-HS (R^2 = 0.88112) also showed statistically significant differences ($p < 0.05$) in "stirring time" and "speed" factors. Smaller particle sizes were observed at higher speed levels. It was noticed that the PSD decreased as the speed levels increased.

3.3. Evaluation of Zeta Potential

In addition to PSD results, complementary processing methods can also influence the interfacial behavior of emulsions (Figure 3). The surfactants in the primary sunscreen emulsion formulation (Potassium Cetyl Phosphate and Sodium Stearoyl Glutamate) induce strong electrostatic repulsion with anionic charges among the particles [42]. Zeta potential is an indicator of physicochemical stability when its absolute value for anionic charges is close to −30 mV [43,44].

At T0 (Figure 3a), the zeta potential of CP-HPH samples appeared more linear, similar to PSD, and even close to the absolute zeta potential value of −30 mV; CP-HPH samples exhibited instability phenomena after exposure conditions at freeze-thaw cycles due to increased PSD caused by low coverage of surfactants on their particles after freeze-thaw cycles, which probably contributed to zeta potential change after freeze-thaw cycles.

CP-HS samples (Figure 3b) with larger particle sizes also exhibited greater electrostatic repulsion between particles, as observed in 1-HS, 2-HS, and 4-HS. Other samples also showed suitable values at T0, indicating electrostatic repulsion and physicochemical stability [45]. Also, CP-HPH and CP-HS emulsions exposed to a "speed" factor of 10,000 and 15,000 rpm or a "stirring time" factor of 15 min had lower zeta potential values after freeze-thaw cycles.

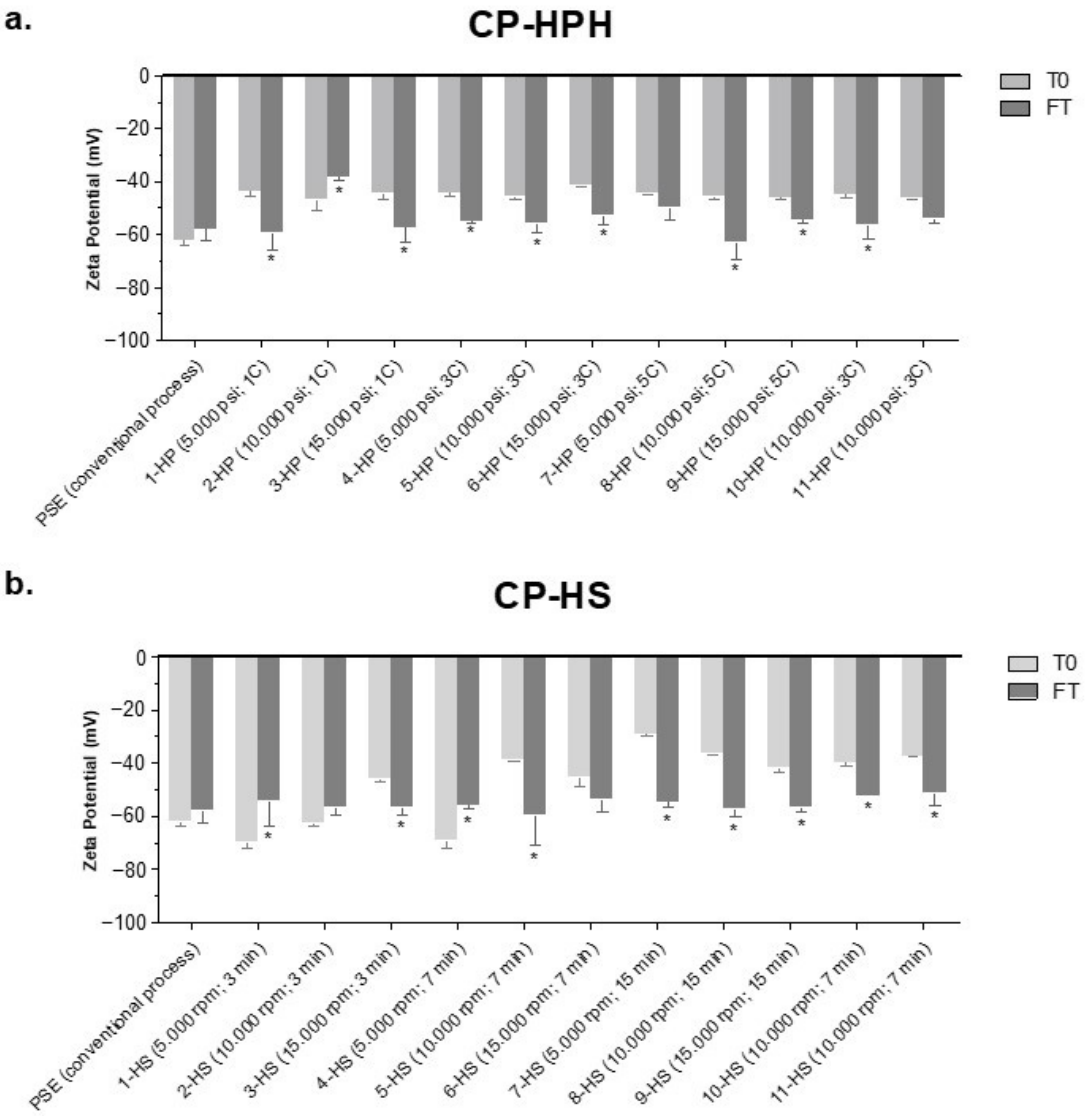


Figure 3. Zeta potential average of emulsions produced by CP-HPH (**a**) and CP-HS (**b**) at initial time (T0) and after 3 freeze-thaw cycles, resulting in 6 days (FT), where $p < 0.05$ is represented by (*). Each process' conditions are indicated in the legend in parentheses, where "C" stands for the number of cycles in CP-HPH.

3.4. Evaluation of pH

The formulations under investigation showed acceptable pH values (Figure 4), considering the type of application, since sunscreen emulsions should have pH levels close to the skin pH (4.6–5.8), aiming to avoid potential dermal irritations. A few assays of CP-HS and CP-HPH presented alterations compared to the primary sunscreen emulsion at T0; only 7-HS, 6-HP, and 9-HP showed statistically significant differences ($p < 0.05$).

There was a pH modification after freeze-thaw cycles compared to T0 in the CP-HPH samples: 3-HP, 4-HP, 5-HP, 9-HP, and 10-HP. In the CP-HS, only 7-HS showed a significant difference between T0 and the freeze-thaw cycle conditions.

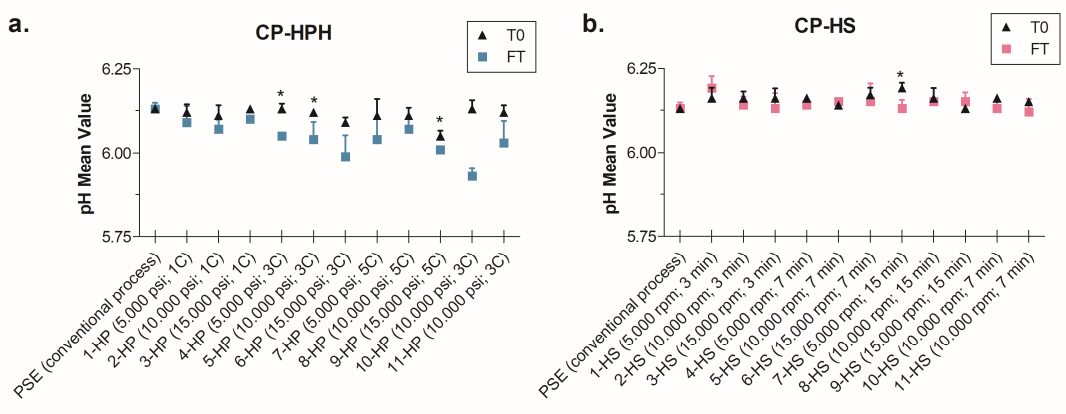


Figure 4. The mean pH values were recorded at the initial time (T0) and after freeze-thaw cycles (FT) for the primary sunscreen emulsion, CP-HS (**a**), and CP-HPH (**b**) assays, with the processing conditions indicated in parentheses, where "C" means the number of cycles in the CP-HPH. Statistically significant differences ($p < 0.05$) between T0 and FT for the same sample are represented by (*).

3.5. Rheological Behavior of Emulsions

All evaluated samples presented pseudoplastic or shear-thinning behavior (n < 1), indicating viscosity changes at determined shear rates, which can influence the distribution of the product under the skin [32].

In the apparent viscosity curves (Figures 5 and 6), the primary sunscreen emulsion at T0 and after freeze-thaw cycles exhibited suitable viscosity characteristics for this type of application. In CP-HPH, only the sample subjected to the less energetic processing method condition, 1-HP, maintained a viscosity like primary sunscreen emulsion at 0.1 s^{-1}, while the other samples showed lower viscosity at T0 and a decrease after freeze-thaw cycles.

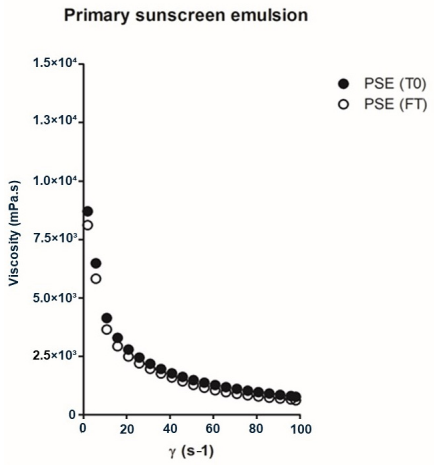


Figure 5. Viscosity curves at 0–100 s^{-1} of primary sunscreen emulsion, represented by PSE, at T0 and after three freeze-thaw cycles, resulting in 6 days (FT).

CP-HS showed higher viscosity than CP-HPH, similar to the primary sunscreen emulsion. After freeze-thaw cycles, unlike CP-HPH and primary sunscreen emulsion, CP-HS assays exhibited a slight increase compared to T0.

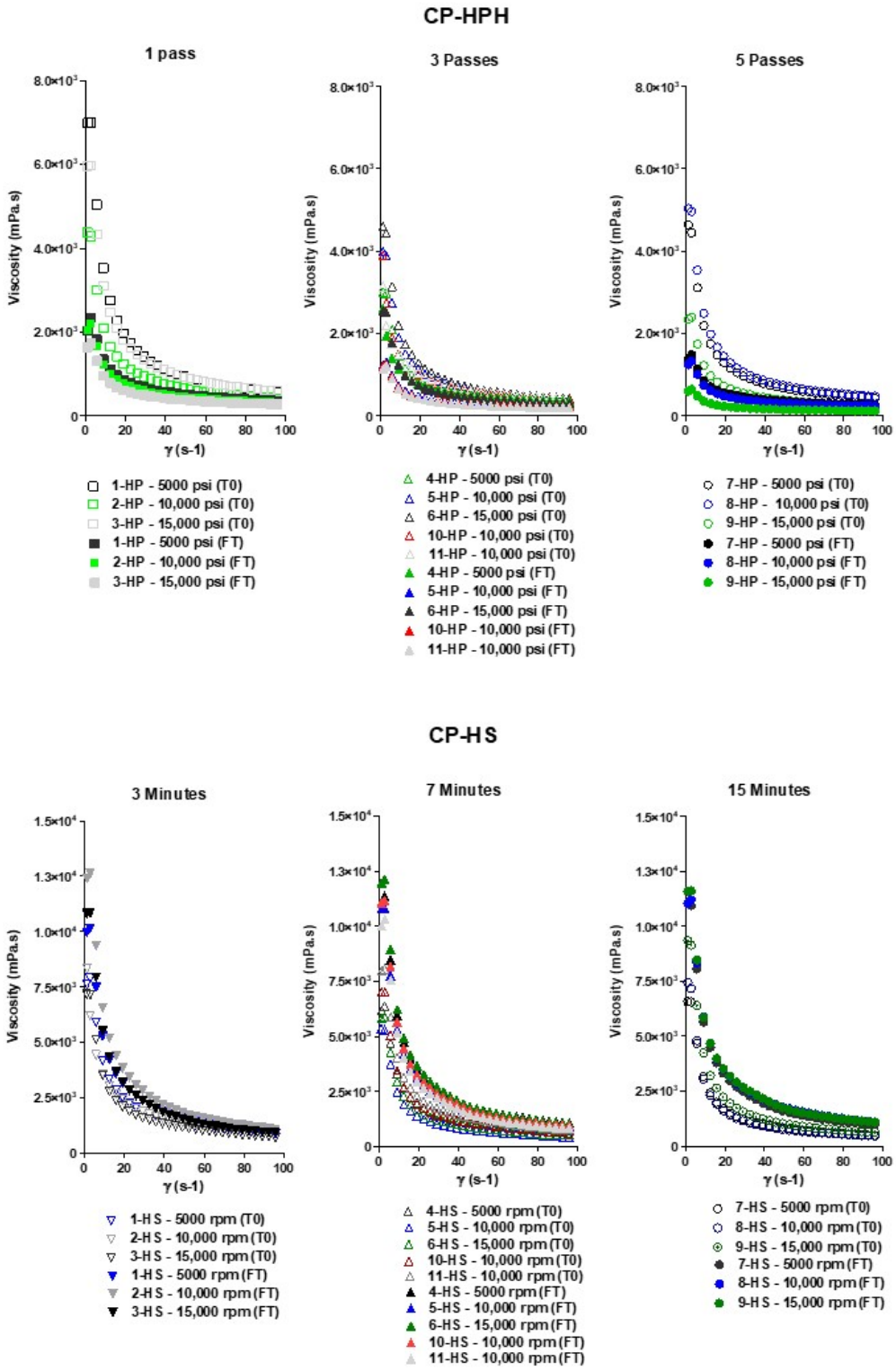


Figure 6. Viscosity curves at 0–100 s^{-1} of CP-HPH, separated by "number of cycles" levels, and CP-HS, separated by "stirring time" levels, at T0 and after three freeze-thaw cycles, resulting in 6 days (FT).

3.6. Evaluation of Photoprotective Property and Photostability

Emulsions produced by CP-HPH exhibit a lower photoprotective property compared to the primary sunscreen emulsion or CP-HS emulsions at T0 (Figure 7a). However, they show less susceptibility to artificial radiation stress (T0 + UV), indicating photostability.

The PSD modification probably influenced the SPF value, as the particle size can affect the properties of organic UV filters [46].

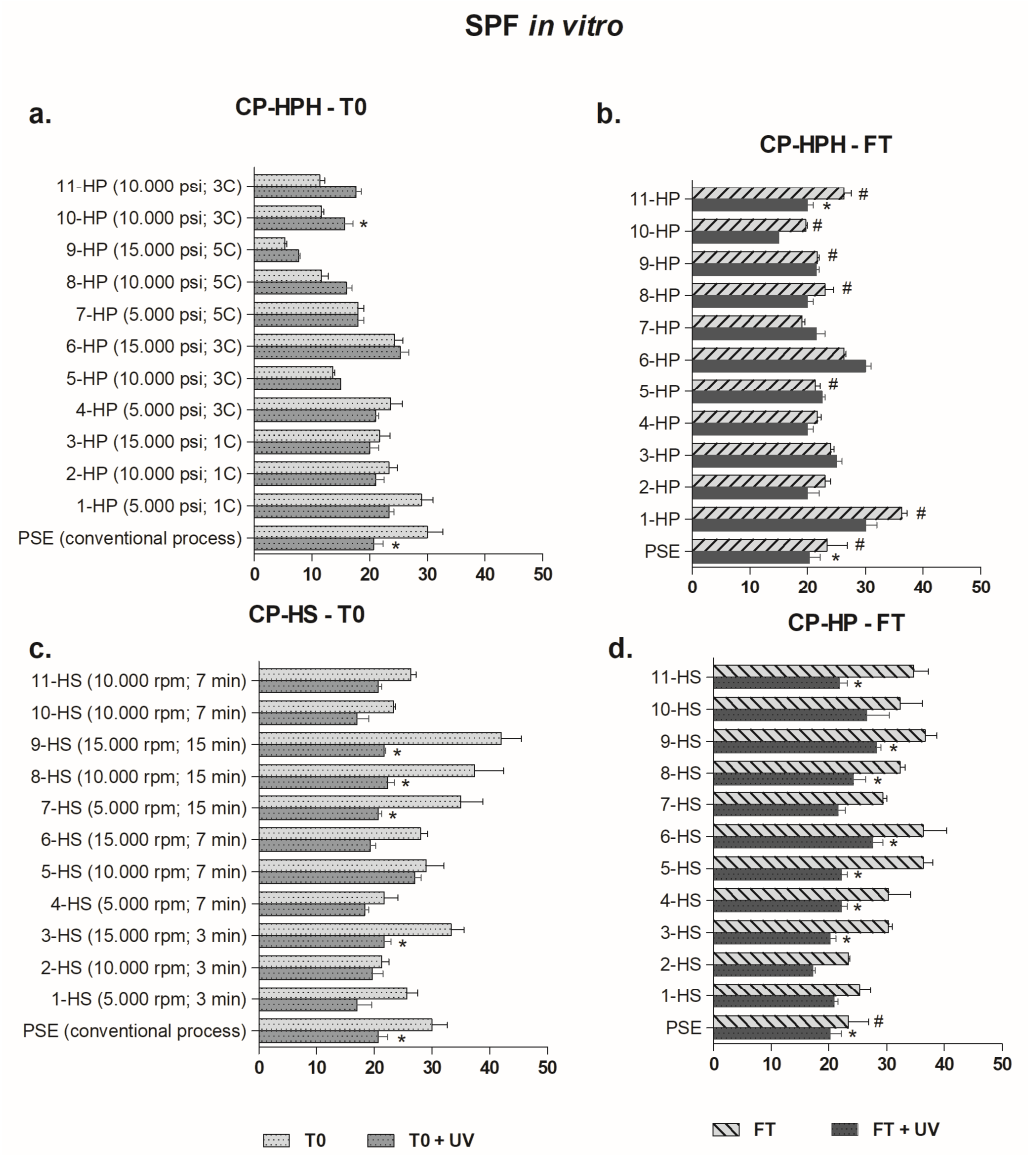


Figure 7. Evaluation of in vitro SPF for primary sunscreen emulsion (PSE), CP-HPH (**a**), and CP-HS (**c**) at the initial time (T0) and after artificial radiation in photostability assay (T0 + UV). Evaluation after three freeze-thaw cycles, resulting in 6 days (FT), and its photostability assay (FT + UV) for CP-HPH (**b**) and CP-HS (**d**). Statistically significant differences ($p < 0.05$) between results before and after the photostability assay for the same sample are represented by (*), and $p < 0.05$ between T0 and after FT for the same sample without artificial radiation are represented by (#). The legend in T0 grap-HS contains, in parentheses, the process conditions used for each method, where "C" means the number of cycles in CP-HPH.

The in vitro SPF of CP-HS at T0 (Figure 7c) showed SPF values ranging from 21—the lowest—to 42—the highest. Subjecting the primary sunscreen emulsion to certain conditions of CP-HS allowed for an increase in SPF, probably due to improved system dispersion and reduced PSD. When employing the highest level of energy during processing, either through "stirring time" or "speed" factors, SPF values were enhanced, as observed in samples 3-HS, 6-HS, 7-HS, 8-HS, and 9-HS. Regarding photostability (T0 + UV), similar to the primary sunscreen emulsion, CP-HS emulsions with higher SPF values exhibited significant alterations ($p < 0.05$) after artificial radiation stress.

The freeze-thaw cycles resulted in higher SPF values for CP-HPH samples compared to those obtained at T0 (Figure 7b). There was a significant difference between T0 and after FT in samples 1HPH, 5HPH, 8HPH, 9HPH, 10HPH, and 11HPH. In the photostability assay (FT + UV), only formulation 11HPH showed a statistically significant difference ($p < 0.05$) compared to T6 without artificial radiation, indicating that most of the CP-HPH samples remained photostable.

All samples in CP-HS remained stable in terms of in vitro SPF freeze-thaw conditions, indicating that photoprotective capacity attributed to the formulations remained stable even after changes in viscosity and PSD (Figure 7d). However, similar to the primary sunscreen emulsion, CP-HS samples underwent photodegradation after artificial radiation (FT + UV).

Each complementary processing method presented distinct advantages, with CP-HS increasing SPF at T0 and maintaining it after freeze-thaw cycles and CP-HPH demonstrating resistance to photodegradation at both times.

4. Discussion

The investigation of the effect of complementary processing methods on the physicochemical properties and photoprotective efficacy of a sunscreen emulsion revealed significant modifications when compared to conventional processes. The PSD has a significant impact on different properties of emulsion systems. When complementary processing methods are employed, particularly those that modify the particle population, physicochemical changes are expected. High-speed and high-pressure methods are effective in inducing PSD refinement in dispersed systems [47,48].

Saavedra et al. (2021) also observed this behavior when comparing the PSD of emulsions processed by high-pressure homogenization and high-shear stirring devices, where was possible to access lower PSD in high-pressure homogenization processing [47]. High-pressure homogenization tends to reduce the particle diameter due to the high shear promoted by the drastic pressure difference during cavitation and also due to collision between the particles of the system [44].

Considering the surface plots, the plateau reached by CP-HPH is described as an event of saturation of the particle reduction power in a system, where an increase in cycles subjects all particles to the same shear force, reaching the maximum limit of PSD reduction [49]. In the CP-HS surface plot, it was possible to reach an optimized condition for achieving a smaller particle size, which was 16,000 rpm for 10 min.

The differences in the PSD results between the studied complementary processing methods reflected the distinct operating principles of each technique. CP-HPH and CP-HS showed a significant reduction in PSD compared to the primary sunscreen emulsion. Ravera et al. (2021) described the composition and application type of an emulsion as essential to determining its processing method [49].

Even though CP-HPH resulted in the smallest PSD, CP-HS presented more stability after freeze-thaw cycles and may be considered a suitable complementary processing method for this emulsion formulation. Higher conditions of "stirring time" or "speed" showed benefits in PSD reduction and other final characteristics, such as SPF in vitro and apparent viscosity. The results of CP-HS showed that an increase in stirring time could be sufficient to improve PSD refinement without necessarily requiring high-speed levels of stirring.

PSD can also be linked with the electrostatic repulsion changes in the complementary processing methods, in which CP-HPH samples presented linear electrostatic repulsion at T0 and less negative than primary sunscreen emulsion, as well as CP-HS samples. Even though the samples are higher than −30 mV, these results can indicate less electrostatic

stability, and emulsions depend on the repulsion forces between their particles, which can delay phenomena such as flocculation and creaming [50].

The observed increase in negative charge in both complementary processing methods after FT may be related to the PSD rise, as observed in other colloidal systems [51,52]. Emulsions exposed to stress conditions after freeze-thaw cycles may have undergone some form of aggregation, which tends to increase electrostatic repulsion. As a result, the amount of surfactant becomes sufficient again to form a film on the particles, facilitating repulsion between particles and reflecting in zeta potential changes [53,54].

Stability tests are crucial to ensure the emulsion system maintains the immiscible phases dispersed during the shelf-life since emulsions are thermodynamically unstable [9]. The physicochemical changes in emulsions exposed to freeze-thaw cycles may be more noticeable than those in other stability assays. The aqueous and oily phase transition between solid and liquid states during freeze-thaw cycles can lead to structural modifications in the dispersion [55].

The instability of CP-HPH by freeze-thaw cycles can be explained by an inverse relation between surfactant concentration in the formulation and the particle distribution, where the smaller particle size needed a superior amount of surfactant to cover all small particle populations [47,56]. The surfactant concentration in ESP, the starting point formulation, was not sufficient to withstand the higher levels of CP-HPH without phase separation after freeze-thaw cycles. Galvão et al. (2018) reported similar results in their research, where freeze-thaw cycles caused noticeable and non-reversible changes in emulsions produced by high-pressure homogenization to phase separation [40]. However, the CP-HPH assay with the lowest "pressure" factor would be sufficient to produce emulsions with a smaller PSD and without phase separation after intense temperature variations proposed by freeze-thaw cycles.

Considered an indicator of stability, pH is one of the attributes that can influence the physicochemical characteristics of emulsions, besides being a property directly correlated to the safe use of topical products [10]. Figure 4 suggests that some processing conditions proposed by CP-HPH and CP-HS after freeze-thaw cycles may have influenced the pH profile. Similar results were observed by Khunkitti et al. (2014), where distinct conditions proposed by changing ingredients in sunscreen emulsions resulted in pH reduction after six freeze-thaw cycles [57].

Despite the modified pH samples, the alterations would be more significant if there were changes in the composition or concentration of the primary sunscreen emulsion formulation, as observed by Zhong et al. (2020) when producing emulsions with different compositions [58].

Intramolecular interactions between ingredients in a formulation as well as complementary processing methods can significantly affect the rheological behavior of samples [59,60]. Additionally, rheological measurements are capable of detecting even the slightest differences among samples [61]. Similar to other physicochemical analyses, the variations introduced by the factorial design of CP-HS and CP-HPH showed contrasts in apparent viscosity, consistency values, and spreadability index in comparison with the primary sunscreen emulsion.

Pseudoplastic behavior, presented in Table 4, is a significant aspect of cosmetics, particularly sunscreen products, as it tends to be accepted by consumers, leading them to use it frequently [62,63]. Oil-in-water emulsions with high quantities of dispersed oil phase, such as sunscreen oil phase with organic UV filters, are often classified as non-Newtonian fluid ($n < 1$). Its pseudoplasticity is related to the packing and ordering of particles under deformation. When the shear rate increases, the particles become more ordered, offering less resistance to the applied force and decreasing the apparent viscosity [32,41].

Table 4. Power law model fitting consistency index (K) and flow behavior (n) of the primary sunscreen emulsion, CP-HS, and CP-HPH at T0 and after freeze-thaw cycles.

Samples	T0			Freeze-Thaw Cycles		
	K (Pa.s^n)	n	R^2	K (Pa.s^n)	n	R^2
Conventional process						
Primary sunscreen emulsion	23.89 ± 2.242	0.2811 ± 0.02383	0.9291	23.96 ± 2.946	0.2381 ± 0.03147	0.8399
CP-HPH						
1-HP (5.000 psi; 1C)	16.360 ± 0.7692	0.2692 ± 0.01184	0.9670	4.204 ± 0.1053	0.4642 ± 0.00607	0.9974
2-HP (10.000 psi; 1C)	8.398 ± 0.2540	0.3413 ± 0.00759	0.9920	3.641 ± 0.1133	0.4725 ± 0.00753	0.9961
3-HP (15.000 psi; 1C)	13.040 ± 0.4764	0.3233 ± 0.00903	0.9867	2.583 ± 0.08017	0.5133 ± 0.00748	0.9968
4-HP (5.000 psi; 3C)	6.224 ± 0.2242	0.3193 ± 0.00898	0.9869	4.327 ± 0.1266	0.4522 ± 0.00710	0.9961
5-HP (10.000 psi; 3C)	7.690 ± 0.2309	0.3470 ± 0.00739	0.9923	1.736 ± 0.1363	0.5589 ± 0.01885	0.9835
6-HP (15.000 psi; 3C)	9.223 ± 0.3257	0.320 ± 0.00880	0.9877	3.819 ± 0.1782	0.4445 ± 0.01134	0.9896
7-HP (5.000 psi; 5C)	8.993 ± 0.2838	0.3375 ± 0.00785	0.9911	2.065 ± 0.1146	0.5593 ± 0.01332	0.9918
8-HP (10.000 psi; 5C)	10.310 ± 0.3765	0.3269 ± 0.00909	0.9872	1.625 ± 0.1253	0.5838 ± 0.01847	0.9855
9-HP (15.000 psi; 5C)	4.730 ± 0.1552	0.3621 ± 0.00813	0.9919	0.605 ± 0.1158	0.6644 ± 0.04550	0.9366
10-HP (10.000 psi; 3C)	8.050 ± 0.1742	0.3520 ± 0.00908	0.9827	1.576 ± 0.1280	0.5674 ± 0.01948	0.9829
11-HP (10.000 psi; 3C)	7.910 ± 0.1359	0.3520 ± 0.00673	0.9903	1.522 ± 0.1165	0.5623 ± 0.01838	0.9844
CP-HS						
1-HS (5.000 rpm; 3 min)	15.900 ± 0.5327	0.3711 ± 0.00829	0.9921	26.640 ± 1.592	0.2646 ± 0.01493	0.9464
2-HS (10.000 rpm; 3 min)	17.080 ± 0.5543	0.3658 ± 0.00797	0.9921	32.710 ± 1.824	0.2553 ± 0.01395	0.9486
3-HS (15.000 rpm; 3 min)	14.810 ± 0.5608	0.3413 ± 0.00933	0.9875	31.500 ± 1.773	0.2504 ± 0.01410	0.9451
4-HS (5.000 rpm; 7 min)	12.530 ± 0.3997	0.3714 ± 0.00783	0.9926	28.610 ± 1.341	0.2870 ± 0.01166	0.9716
5-HS (10.000 rpm; 7 min)	10.690 ± 0.4558	0.3131 ± 0.01065	0.9807	26.250 ± 1.335	0.2625 ± 0.01272	0.9590
6-HS (15.000 rpm; 7 min)	13.150 ± 0.6038	0.2992 ± 0.01150	0.9755	30.690 ± 1.619	0.2637 ± 0.01318	0.9568
7-HS (5.000 rpm; 15 min)	15.330 ± 0.7373	0.2511 ± 0.01204	0.9591	29.340 ± 1.488	0.2755 ± 0.01264	0.9638
8-HS (10.000 rpm; 15 min)	15.380 ± 0.6970	0.2337 ± 0.01139	0.9558	26.260 ± 1.218	0.2953 ± 0.01152	0.9739
9-HS (15.000 rpm; 15 min)	20.590 ± 1.0110	0.2381 ± 0.01233	0.9508	27.970 ± 1.232	0.3059 ± 0.01092	0.9782
10-HS (10.000 rpm; 7 min)	14.460 ± 0.5999	0.3231 ± 0.01026	0.9827	27.480 ± 1.390	0.2581 ± 0.01265	0.9578
11-HS (10.000 rpm; 7 min)	16.580 ± 0.8136	0.3355 ± 0.01211	0.9781	26.230 ± 1.495	0.2473 ± 0.01428	0.9422

Legend: "C" represents the number of cycles in CP-HPH.

The viscosity loss observed in CP-HPH may be associated with the homogenization method employed by HPH (Figure 6). The high shear promoted by HPH can lead to the breakdown of macromolecules that control the apparent viscosity. The mechanical force exerted by a high-pressure piston, followed by passage through a small gap, facilitates the breakdown of macromolecules [64]. Xanthan gum and polyacrylate cross polymer-11, used in primary sunscreen emulsion formulation to increase apparent viscosity and modify sensory aspects, probably suffered structural modifications during the CP-HPH process [9].

The PSD of fluid particles can influence the shear stress and apparent viscosity, especially in the case of non-Newtonian fluids [65,66]. Pal (2000) reported that smaller particles with a higher number in emulsified systems result in higher apparent viscosity, reinforcing the findings for CP-HS [54]. Nevertheless, in the case of CP-HPH, where the samples had the smallest PSD, the breakdown of polymers prevented an apparent viscosity increase.

When comparing the complementary processing methods, it was observed that CP-HS maintained an apparent viscosity similar to that of the primary sunscreen emulsion, indicating that the high-shear (rotor-stator) principle did not negatively influence this characteristic. While in CP-HPH, intramolecular changes related to the amount of anionic surfactant, oil phase ratio, and polymers were sufficient to modify significantly the apparent viscosity in all assays. Techniques to assess rheological parameters are essential for

understanding the physicochemical instability phenomena in CP-HPH. Zhou et al. (2022) observed that emulsions obtained via high-pressure homogenization presented a lower apparent viscosity than emulsions obtained through high-shear (rotor-stator) homogenization, and the consistency index (K) also confirmed the same behavior, being lower in the first case [28].

Photochemical and photophysical interactions between the combination of UV filters and other components of sunscreen composition define the photoprotective properties of the final product [67]. The composition of primary sunscreen emulsion consisted of a mixture of organic UV filters with absorbance profiles in the UVA region, such as Hydroxybenzoyl Hexyl Benzoate (DHHB), as well as UVB filters, like Ethylhexyl Methoxycinnamate (EHMC), and broad-spectrum filters like Butyl Methoxydibenzoylmethane (BMDBM) and Ethylhexyloxyphenol Methoxyphenyl Triazine (BEMT). It is important to note that organic UV filters that are composed of primary sunscreen emulsion formulation are insoluble in water, have low solubility in oils, and considerable amounts are required for suitable dispersion in the emulsion to achieve photoprotective action [68,69].

Considering that filters are challenging to disperse in emulsion systems, CPMs can facilitate dispersion and homogenization as an alternative to enhance this application. According to Herzog et al. (2015), all systems composed of the dispersion of UV filters have their efficiency evaluated by light scattering techniques, where the size and distribution of dispersed particles can influence efficacy, like the SPF [46]. The emulsions developed in this study, which passed through different processes and acquired distinct physicochemical characteristics, also demonstrated statistically significant differences in in vitro SPF before and after exposure to artificial sun radiation (Figure 7).

Additionally, it is important to take into consideration the difference in rheological behavior when compared to the primary sunscreen emulsion. Properties such as viscosity, texture, adhesiveness, and spreadability can have an impact on the SPF in sunscreen emulsions [57]. Due to its high homogenization capacity, HPH is a technique recommended for obtaining emulsion systems on a nanometric scale [26]. However, a negative effect of this technique was observed in maintaining or enhancing the in vitro SPF value under the conditions studied in the factorial design.

On the other hand, in CP-HPH, formulations with more energetic processing showed lower SPF values, except for 6-HP. Due to the complexity of the system, variations in SPF may extend beyond the choice of UV filters in its composition. Changes can be attributed to the physicochemical characteristics of the emulsion, rheological properties, and even the ability to form a film during application on the skin or the PMMA plate [70,71].

Both complementary processing methods showed an inversely proportional relationship at T0. In the case of CP-HS, formulations that required more energy in terms of stirring time and speed had higher SPF, while CP-HPH presented higher SPF in samples that required lower energy in terms of pressure and number of cycles.

The increase in SPF after freeze-thaw cycles in CP-HPH is probably due to particle size and the signs of physicochemical instability after freeze-thaw cycles. What was evaluated at FT was larger particles in the oily phase, favoring the deposition of a higher charge of UV filters on the PMMA substrate compared to T0. This change may have contributed to the increase in SPF after freeze-thaw cycles.

Although SPF has lower values after exposure to artificial radiation, Wypych (2015) considered that a sunscreen formulation can still be suitable for use even if it shows a short level of photodegradation because the components of the formulation have an action for a determined exposure time, and the product reapplication should be every two hours [72].

These results emphasize the importance of the appropriate choice of processing method and formulation ingredients to obtain high-quality and effective sunscreen emulsions.

5. Conclusions

The complementary processing methods, CP-HPH and CP-HS, can influence the final characteristics of the emulsion, including the PSD, zeta potential, rheological properties, and photoprotective profiles. The selection of processing methods is essential for developing emulsions with physicochemical stability and efficacy. CP-HS, in addition to generating fine and uniform particles, increases in vitro SPF. CP-HPH, on the other hand, resulted in more refined PSD and photostability properties despite showing signs of instability due to surfactant concentration in the primary sunscreen emulsion formulation. Our study provides practical insights that are relevant to a range of industries, in particular the cosmetic industry, which will have the benefit of a more ascertained method for the development of new emulsified systems.

Author Contributions: Conceptualization, Y.R.S. and V.R.L.-S.; methodology, Y.R.S., N.A.-F., P.S.L., D.R.A., A.F.S., C.C.S., A.R.B., M.D.D. and V.R.L.-S.; software, Y.R.S.; M.D.D.; formal analysis, Y.R.S., N.A.-F., D.R.A., A.F.S., C.C.S., A.R.B., M.D.D., V.R.L.-S.; data curation, Y.R.S., N.A.-F., D.R.A., A.F.S., M.D.D., V.R.L.-S.; writing—original draft preparation Y.R.S.; writing—review and editing, N.A.-F., P.S.L., D.R.A., A.R.B., M.D.D., V.R.L.-S.; supervision, M.D.D., V.R.L.-S.; project administration, Y.R.S., V.R.L.-S. All authors have read and agreed to the published version of the manuscript.

Funding: A.R.B. is highly thankful to the Conselho Nacional de Desenvolvimento Científico e Tecnológico, CNPq, for the Research Productivity Scholarship (CNPq, Process 303862/2022-0), and to Fundação de Amparo à Pesquisa do Estado de São Paulo (FAPESP, processes 2008/57800-0 and 2012/04435-9). Vania R Leite-Silva is highly thankful to the Conselho Nacional de Desenvolvimento Científico e Tecnológico, CNPq, for the Productivity Scholarship in Technological Development and Extension Innovation—DT (CNPq, Process 302153/2023-3), and to Fundação de Amparo à Pesquisa do Estado de São Paulo (FAPESP, process 2024/12480-1).

Data Availability Statement: Data are contained within the article.

Conflicts of Interest: The authors declare no conflicts of interest.

References

1. Bałdyga, J.; Jasińska, M.; Kowalski, A.J. Effect of Rheology of Dense Emulsions on the Flow Structure in Agitated Systems. *Chem. Eng. Res. Des.* **2016**, *108*, 3–12. [CrossRef]
2. Ho, T.M.; Razzaghi, A.; Ramachandran, A.; Mikkonen, K.S. Emulsion Characterization via Microfluidic Devices: A Review on Interfacial Tension and Stability to Coalescence. *Adv. Colloid Interface Sci.* **2022**, *299*, 102541. [CrossRef] [PubMed]
3. Yamashita, Y.; Miyahara, R.; Sakamoto, K. Emulsion and Emulsification Technology. In *Cosmetic Science and Technology: Theoretical Principles and Applications*; Elsevier Inc.: Amsterdam, The Netherlands, 2017; pp. 489–506, ISBN 9780128020548.
4. Hu, Y.T.; Ting, Y.; Hu, J.Y.; Hsieh, S.C. Techniques and Methods to Study Functional Characteristics of Emulsion Systems. *J. Food Drug Anal.* **2017**, *25*, 16–26. [CrossRef] [PubMed]
5. Calixto, L.S.; Maia Campos, P.M.B.G. Physical–Mechanical Characterization of Cosmetic Formulations and Correlation between Instrumental Measurements and Sensorial Properties. *Int. J. Cosmet. Sci.* **2017**, *39*, 527–534. [CrossRef] [PubMed]
6. Khanum, R.; Thevanayagam, H. Lipid Peroxidation: Its Effects on the Formulation and Use of Pharmaceutical Emulsions. *Asian J. Pharm. Sci.* **2017**, *12*, 401–411. [CrossRef] [PubMed]
7. Al-Bawab, A.; Friberg, S.E. Some Pertinent Factors in Skin Care Emulsion. *Adv. Colloid Interface Sci.* **2006**, *123–126*, 313–322. [CrossRef] [PubMed]
8. Yamashita, Y.; Sakamoto, K. Structural Analysis of Formulations. In *Cosmetic Science and Technology: Theoretical Principles and Applications*; Elsevier Inc.: Amsterdam, The Netherlands, 2017; pp. 635–655, ISBN 9780128020548.
9. Tadros, T.F. *Emulsion Formation, Stability, and Rheology*; John Wiley & Sons, Inc.: Hoboken, NJ, USA, 2013.
10. Dickinson, E. Strategies to Control and Inhibit the Flocculation of Protein-Stabilized Oil-in-Water Emulsions. *Food Hydrocoll.* **2019**, *96*, 209–223. [CrossRef]
11. Pérez-Mosqueda, L.M.; Trujillo-Cayado, L.A.; Carrillo, F.; Ramírez, P.; Muñoz, J. Formulation and Optimization by Experimental Design of Eco-Friendly Emulsions Based on d-Limonene. *Colloids Surf. B Biointerfaces* **2015**, *128*, 127–131. [CrossRef] [PubMed]
12. Singh, Y.; Meher, J.G.; Raval, K.; Khan, F.A.; Chaurasia, M.; Jain, N.K.; Chourasia, M.K. Nanoemulsion: Concepts, Development and Applications in Drug Delivery. *J. Control. Release* **2017**, *252*, 28–49. [CrossRef]

13. Yang, J.; Gu, Z.; Cheng, L.; Li, Z.; Li, C.; Ban, X.; Hong, Y. Preparation and Stability Mechanisms of Double Emulsions Stabilized by Gelatinized Native Starch. *Carbohydr. Polym.* **2021**, *262*, 117926. [CrossRef]
14. Li, H.; Li, F.; Wu, X.; Wu, W. Effect of Rice Bran Rancidity on the Emulsion Stability of Rice Bran Protein and Structural Characteristics of Interface Protein. *Food Hydrocoll.* **2021**, *121*, 107006. [CrossRef]
15. Jin, Y.; Liu, D.; Hu, J. Effect of Surfactant Molecular Structure on Emulsion Stability Investigated by Interfacial Dilatational Rheology. *Polymers* **2021**, *13*, 1127. [CrossRef] [PubMed]
16. Sharkawy, A.; Barreiro, M.F.; Rodrigues, A.E. New Pickering Emulsions Stabilized with Chitosan/Collagen Peptides Nanoparticles: Synthesis, Characterization and Tracking of the Nanoparticles after Skin Application. *Colloids Surf. A Physicochem. Eng. Asp.* **2021**, *616*, 126327. [CrossRef]
17. Franzol, A.; Banin, T.M.; Brazil, T.R.; Rezende, M.C. Assessment of Kinetic Stability of Cosmetic Emulsions Formulated with Different Emulsifiers Using Rheological and Sensory Analyses. *J. Solgel Sci. Technol.* **2021**, *99*, 469–481. [CrossRef]
18. Kovács, A.; Erös, I.; Csóka, I. Optimization and Development of Stable w/o/w Cosmetic Multiple Emulsions by Means of the Quality by Design Approach. *Int. J. Cosmet. Sci.* **2016**, *38*, 128–138. [CrossRef] [PubMed]
19. McClements, D.J. Critical Review of Techniques and Methodologies for Characterization of Emulsion Stability. *Crit. Rev. Food Sci. Nutr.* **2007**, *47*, 611–649. [CrossRef] [PubMed]
20. Rueger, P.E.; Calabrese, R.V. Dispersion of Water into Oil in a Rotor-Stator Mixer. Part 1: Drop Breakup in Dilute Systems. *Chem. Eng. Res. Des.* **2013**, *91*, 2122–2133. [CrossRef]
21. Gutiérrez, J.M.; González, C.; Maestro, A.; Solè, I.; Pey, C.M.; Nolla, J. Nano-Emulsions: New Applications and Optimization of Their Preparation. *Curr. Opin. Colloid Interface Sci.* **2008**, *13*, 245–251. [CrossRef]
22. McClements, D.J.; Jafari, S.M. Improving Emulsion Formation, Stability and Performance Using Mixed Emulsifiers: A Review. *Adv. Colloid Interface Sci.* **2018**, *251*, 55–79. [CrossRef]
23. Zhang, J.; Xu, S.; Li, W. High Shear Mixers: A Review of Typical Applications and Studies on Power Draw, Flow Pattern, Energy Dissipation and Transfer Properties. *Chem. Eng. Process. Process Intensif.* **2012**, *57–58*, 25–41. [CrossRef]
24. Jasińska, M.; Bałdyga, J.; Cooke, M.; Kowalski, A.J. Specific Features of Power Characteristics of In-Line Rotor-Stator Mixers. *Chem. Eng. Process. Process Intensif.* **2015**, *91*, 43–56. [CrossRef]
25. Lee, L.; Hancocks, R.; Noble, I.; Norton, I.T. Production of Water-in-Oil Nanoemulsions Using High Pressure Homogenisation: A Study on Droplet Break-Up. *J. Food Eng.* **2014**, *131*, 33–37. [CrossRef]
26. Håkansson, A. A Hydrodynamic Comparisons of Two Different High-Pressure Homogenizer Valve Design Principles: A Step towards Increased Efficiency. *Chem. Eng. Res. Des.* **2022**, *184*, 303–314. [CrossRef]
27. Stang, M.; Schuchmann, H.; Schubert, H. Emulsification in High-Pressure Homogenizers. *Eng. Life Sci.* **2001**, *1*, 151–157. [CrossRef]
28. Zhou, L.; Zhang, W.; Wang, J.; Zhang, R.; Zhang, J. Comparison of Oil-in-Water Emulsions Prepared by Ultrasound, High-Pressure Homogenization and High-Speed Homogenization. *Ultrason. Sonochem.* **2022**, *82*, 105885. [CrossRef] [PubMed]
29. Rolim Baby, A.; Alberto Haroutiounian-Filho, C.; Daud Sarruf, F.; Roberto Tavante-Júnior, C.; Aparecida Sales de Oliveira Pinto, C.; Zague, V.; Pinheiro Gomes Arêas, E.; Mary Kaneko, T.; Valéria Robles Velasco, M. *Estabilidade e Estudo de Penetração Cutânea in Vitro Da Rutina Veiculada Em Uma Emulsão Cosmética Através de Um Modelo de Biomembrana Alternativo*; Rev. Bras. Cienc. Farm.: São Paulo, Brazil, 2008; Volume 44.
30. Terescenco, D.; Picard, C.; Clemenceau, F.; Grisel, M.; Savary, G. Influence of the Emollient Structure on the Properties of Cosmetic Emulsion Containing Lamellar Liquid Crystals. *Colloids Surf. A Physicochem. Eng. Asp.* **2018**, *536*, 10–19. [CrossRef]
31. Battaglia, L.; Trotta, M.; Gallarate, M.; Carlotti, M.E.; Zara, G.P.; Bargoni, A. Solid Lipid Nanoparticles Formed by Solvent-in-Water Emulsion-Diffusion Technique: Development and Influence on Insulin Stability. *J. Microencapsul.* **2007**, *24*, 672–684. [CrossRef]
32. Kundu, P.; Kumar, V.; Mishra, I.M. Modeling the Steady-Shear Rheological Behavior of Dilute to Highly Concentrated Oil-in-Water (o/w) Emulsions: Effect of Temperature, Oil Volume Fraction and Anionic Surfactant Concentration. *J. Pet. Sci. Eng.* **2015**, *129*, 189–204. [CrossRef]
33. Hübner, A.A.; Demarque, D.P.; Lourenço, F.R.; Rosado, C.; Baby, A.R.; Kikuchi, I.S.; Bacchi, E.M. Phytocompounds Recovered from the Waste of Cabernet Sauvignon (*Vitis vinifera* L.) Vinification: Cytotoxicity (in Normal and Stressful Conditions) and In Vitro Photoprotection Efficacy in a Sunscreen System. *Cosmetics* **2023**, *10*, 2. [CrossRef]
34. Cândido, T.M.; Ariede, M.B.; Pinto, C.A.S.d.O.; Lourenço, F.R.; Rosado, C.; Velasco, M.V.R.; Baby, A.R. Prospecting In Vitro Antioxidant and Photoprotective Properties of Rosmarinic Acid in a Sunscreen System Developed by QbD Containing Octyl P-Methoxycinnamate and Bemotrizinol. *Cosmetics* **2022**, *9*, 29. [CrossRef]
35. Wróblewska, K.B.; Baby, A.R.; Grombone Guaratini, M.T.; Moreno, P.R.H. In Vitro Antioxidant and Photoprotective Activity of Five Native Brazilian Bamboo Species. *Ind. Crops Prod.* **2019**, *130*, 208–215. [CrossRef]
36. Mcclements, D.J. Colloidal Basis of Emulsion Color. *Curr. Opin. Colloid Interface Sci.* **2002**, *7*, 451–455. [CrossRef]
37. Degner, B.M.; Chung, C.; Schlegel, V.; Hutkins, R.; Mcclements, D.J. Factors Influencing the Freeze-Thaw Stability of Emulsion-Based Foods. *Compr. Rev. Food Sci. Food Saf.* **2014**, *13*, 98–113. [CrossRef]

38. Qian, C.; McClements, D.J. Formation of Nanoemulsions Stabilized by Model Food-Grade Emulsifiers Using High-Pressure Homogenization: Factors Affecting Particle Size. *Food Hydrocoll.* **2011**, *25*, 1000–1008. [CrossRef]
39. Salvia-Trujillo, L.; Rojas-Graü, M.A.; Soliva-Fortuny, R.; Martín-Belloso, O. Effect of Processing Parameters on Physicochemical Characteristics of Microfluidized Lemongrass Essential Oil-Alginate Nanoemulsions. *Food Hydrocoll.* **2013**, *30*, 401–407. [CrossRef]
40. Galvão, K.C.S.; Vicente, A.A.; Sobral, P.J.A. Development, Characterization, and Stability of O/W Pepper Nanoemulsions Produced by High-Pressure Homogenization. *Food Bioprocess Technol.* **2018**, *11*, 355–367. [CrossRef]
41. McClements, D.J. *Food Emulsions: Principles, Practices, and Techniques*; Taylor & Francis Group: Abingdon, UK, 2016; Volume 3, ISBN 9781498726696.
42. Niu, H.; Wang, W.; Dou, Z.; Chen, X.; Chen, X.; Chen, H.; Fu, X. Multiscale Combined Techniques for Evaluating Emulsion Stability: A Critical Review. *Adv. Colloid Interface Sci.* **2023**, *311*, 102813. [CrossRef]
43. Asfour, M.H.; Kassem, A.A.; Salama, A. Topical Nanostructured Lipid Carriers/Inorganic Sunscreen Combination for Alleviation of All-Trans Retinoic Acid-Induced Photosensitivity: Box-Behnken Design Optimization, in Vitro and in Vivo Evaluation. *Eur. J. Pharm. Sci.* **2019**, *134*, 219–232. [CrossRef]
44. Joseph, E.; Singhvi, G. Multifunctional Nanocrystals for Cancer Therapy: A Potential Nanocarrier. In *Nanomaterials for Drug Delivery and Therapy*; Elsevier: Amsterdam, The Netherlands, 2019; pp. 91–116, ISBN 9780128165058.
45. Seixas, V.C.; Serra, O.A. Stability of Sunscreens Containing CePO4: Proposal for a New Inorganic UV Filter. *Molecules* **2014**, *19*, 9907–9925. [CrossRef] [PubMed]
46. Herzog, B.; Sengün, F. Scattering Particles Increase Absorbance of Dyes-a Model Study with Relevance for Sunscreens. *Photochem. Photobiol. Sci.* **2015**, *14*, 2054–2063. [CrossRef] [PubMed]
47. Saavedra Isusi, G.I.; Lohner, N.; Karbstein, H.P.; van der Schaaf, U.S. Emulsions Stabilised with Pectin-Based Microgels: Investigations into the Break-up of Droplets in the Presence of Microgels. *J. Food Eng.* **2021**, *294*, 110421. [CrossRef]
48. Walstra, P. 8 Emulsions. In *Fundamentals of Interface and Colloid Science*; Elsevier: Amsterdam, The Netherlands, 2005.
49. Ravera, F.; Dziza, K.; Santini, E.; Cristofolini, L.; Liggieri, L. Emulsification and Emulsion Stability: The Role of the Interfacial Properties. *Adv. Colloid Interface Sci.* **2021**, *288*, 102344. [CrossRef] [PubMed]
50. Cabrera-Trujillo, M.A.; Filomena-Ambrosio, A.; Quintanilla-Carvajal, M.X.; Sotelo-Díaz, L.I. Stability of Low-Fat Oil in Water Emulsions Obtained by Ultra Turrax, Rotor-Stator and Ultrasound Homogenization Methods. *Int. J. Gastron. Food Sci.* **2018**, *13*, 58–64. [CrossRef]
51. Lee, J.H.; Kim, K.; Jin, X.; Kim, T.M.; Choi, I.G.; Choi, J.W. Formation of Pure Nanoparticles with Solvent-Fractionated Lignin Polymers and Evaluation of Their Biocompatibility. *Int. J. Biol. Macromol.* **2021**, *183*, 660–667. [CrossRef]
52. Hyam, R.S.; Subhedar, K.M.; Pawar, S.H. Effect of Particle Size Distribution and Zeta Potential on the Electrophoretic Deposition of Boron Films. *Colloids Surf. A Physicochem. Eng. Asp.* **2008**, *315*, 61–65. [CrossRef]
53. Liu, W.; Sun, D.; Li, C.; Liu, Q.; Xu, J. Formation and Stability of Paraffin Oil-in-Water Nano-Emulsions Prepared by the Emulsion Inversion Point Method. *J. Colloid Interface Sci.* **2006**, *303*, 557–563. [CrossRef]
54. Pal, R. Shear Viscosity Behavior of Emulsions of Two Immiscible Liquids. *J. Colloid Interface Sci.* **2000**, *225*, 359–366. [CrossRef] [PubMed]
55. Taarji, N.; Bouhoute, M.; Melanie, H.; Hafidi, A.; Kobayashi, I.; Neves, M.; Tominaga, K.; Isoda, H.; Nakajima, M. Stability Characteristics of O/W Emulsions Prepared Using Purified Glycyrrhizin or a Non-Purified Glycyrrhizin-Rich Extract from Liquorice Root (*Glycyrrhiza Glabra*). *Colloids Surf. A Physicochem. Eng. Asp.* **2020**, *614*, 126006. [CrossRef]
56. iyer, v.; cayatte, c.; guzman, b.; schneider-Ohrum, K.; Matuszak, R.; Snell, A.; Rajani, G.M.; McCarthy, M.P.; Muralidhara, B. Impact of Formulation and Particle Size on Stability and Immunogenicity of Oil-in-Water Emulsion Adjuvants. *Hum. Vaccines Immunother.* **2015**, *11*, 1853–1864. [CrossRef]
57. Khunkitti, W.; Satthanakul, P.; Waranuch, N.; Pitaksuteepong, T.; Kitikhun, P. Method for screening sunscreen cream formulations by determination of in vitro SPF and PA values using UV transmission spectroscopy and tex-ture profile analysis. *J. Cosmet. Sci.* **2022**, *65*, 147–159.
58. Zhong, Y.; Xiang, X.; Wang, X.; Zhang, Y.; Hu, M.; Chen, T.; Liu, C. Fabrication and Characterization of Oil-in-Water Emulsions Stabilized by Macadamia Protein Isolate/Chitosan Hydrochloride Composite Polymers. *Food Hydrocoll.* **2020**, *103*, 105655. [CrossRef]
59. Vigato, A.A.; Machado, I.P.; Del Valle, M.; da Ana, P.A.; Sepulveda, A.F.; Yokaichiya, F.; Franco, M.K.K.D.; Loiola, M.C.; Tófoli, G.R.; Cereda, C.M.S.; et al. Monoketonic Curcuminoid-Lidocaine Co-Deliver Using Thermosensitive Organogels: From Drug Synthesis to Epidermis Structural Studies. *Pharmaceutics* **2022**, *14*, 293. [CrossRef] [PubMed]
60. Gilbert, L.; Savary, G.; Grisel, M.; Picard, C. Predicting Sensory Texture Properties of Cosmetic Emulsions by Physical Measurements. *Chemom. Intell. Lab. Syst.* **2013**, *124*, 21–31. [CrossRef]
61. Moravkova, T.; Filip, P. Relation between Sensory Analysis and Rheology of Body Lotions. *Int. J. Cosmet. Sci.* **2016**, *38*, 558–566. [CrossRef] [PubMed]

62. Lukic, M.; Jaksic, I.; Krstonosic, V.; Cekic, N.; Savic, S. A Combined Approach in Characterization of an Effective w/o Hand Cream: The Influence of Emollient on Textural, Sensorial and in Vivo Skin Performance. *Int. J. Cosmet. Sci.* **2012**, *34*, 140–149. [CrossRef]
63. Cozzi, A.C.; Perugini, P.; Gourion-Arsiquaud, S. Comparative Behavior between Sunscreens Based on Free or Encapsulated UV Filters in Term of Skin Penetration, Retention and Photo-Stability. *Eur. J. Pharm. Sci.* **2018**, *121*, 309–318. [CrossRef]
64. Wei, B.; Cai, C.; Jin, Z.; Tian, Y. High-Pressure Homogenization Induced Degradation of Amylopectin in a Gelatinized State. *Starch/Staerke* **2016**, *68*, 734–741. [CrossRef]
65. Braisch, B.; Köhler, K.; Schuchmann, H.P.; Wolf, B. Preparation and Flow Behaviour of Oil-in-Water Emulsions Stabilised by Hydrophilic Silica Particles. *Chem. Eng. Technol.* **2009**, *32*, 1107–1112. [CrossRef]
66. Derkach, S.R. Rheology of Emulsions. *Adv. Colloid Interface Sci.* **2009**, *151*, 1–23. [CrossRef] [PubMed]
67. Bonda, C.A.; Lott, D. Sunscreen Photostability. In *Principles and Practice of Photoprotection*; Springer International Publishing: Berlin/Heidelberg, Germany, 2016; pp. 247–273, ISBN 9783319293820.
68. Sauce, R.; Pinto, C.A.S.d.O.; Velasco, M.V.R.; Rosado, C.; Baby, A.R. Ex Vivo Penetration Analysis and Anti-Inflammatory Efficacy of the Association of Ferulic Acid and UV Filters. *Eur. J. Pharm. Sci.* **2021**, *156*, 105578. [CrossRef]
69. Herzog, B.; Quass, K.; Schmidt, E.; Müller, S.; Luther, H. Physical Properties of Organic Particulate UV Absorbers Used in Sunscreens: II. UV-Attenuating Efficiency as Function of Particle Size. *J. Colloid Interface Sci.* **2004**, *276*, 354–363. [CrossRef]
70. Hewitt, J.P. Sunscreen Formulation: Optimising Aesthetic Elements for Twenty-First-Century Consumers. In *Principles and Practice of Photoprotection*; Springer International Publishing: Berlin/Heidelberg, Germany, 2016; pp. 289–302, ISBN 9783319293820.
71. Daly, S.; Ouyang, H.; Maitra, P. Chemistry of Sunscreens. In *Principles and Practice of Photoprotection*; Springer International Publishing: Berlin/Heidelberg, Germany, 2016; pp. 159–178, ISBN 9783319293820.
72. Wypych, G. (Ed.) *Handbook of UV Degradation and Stabilization*, 2nd ed.; ChemTec Publising: Toronto, ON, Canada, 2015; Volume 1, ISBN 9781895198867.

Disclaimer/Publisher's Note: The statements, opinions and data contained in all publications are solely those of the individual author(s) and contributor(s) and not of MDPI and/or the editor(s). MDPI and/or the editor(s) disclaim responsibility for any injury to people or property resulting from any ideas, methods, instructions or products referred to in the content.